Hydrogen Bond Dynamics of Methyl Acetate in Methanol

ARTICLE *in* JOURNAL OF PHYSICAL CHEMISTRY LETTERS · OCTOBER 2010

Impact Factor: 7.46 · DOI: 10.1021/jz1010994

THE JOURNAL OF PHYSICAL CHEMISTRY Letters

pubs.acs.org/JPCL

Hydrogen Bond Dynamics of Methyl Acetate in Methanol

Marco Pagliai,[†] Francesco Muniz-Miranda,[‡] Gianni Cardini,*[,†,‡] Roberto Righini,[†,‡] and Vincenzo Schettino[†,‡]

[†]Dipartimento di Chimica, Università degli Studi di Firenze, via della Lastruccia 3, 50019 Sesto Fiorentino (Firenze), Italia, and [‡]European Laboratory for Nonlinear Spectroscopy (LENS), via Nello Carrara 1, 50019 Sesto Fiorentino (Firenze), Italia

ABSTRACT The H-bond interactions of methyl acetate in methanol have been studied by means of ab initio molecular dynamics simulations within the Car−Parrinello approach. It has been observed that the C═O stretching band of methyl acetate splits into a doublet as a consequence of the interaction with the solvent. The H-bond effects on the spectroscopic properties of methyl acetate in methanol have been interpreted by wavelet transform analysis in conjunction with a structural and dynamic characterization of the solvation cage. Localizing a vibrational mode in time and frequency during the simulations has allowed association of the different interactions with the solvent to the vibrational properties. This represents an important development in the capability of molecular dynamics simulations to explain experimental data obtained by time-resolved spectroscopic methods.

SECTION Kinetics, Spectroscopy

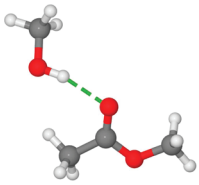

Two of the most useful approaches to characterize structural and spectroscopic properties related to the H-bond interaction are time-resolved spectroscopy, in particular, two-dimensional infrared (2D IR) spectroscopy,[1−5] and molecular dynamics simulations,[6] especially in the Car−Parrinello approach.[7−10] In order to obtain useful insight into the H-bond dynamics, it is important to establish the correlation between structural and vibrational properties in simulations and to compare the results with experimental measurements. This can be achieved by adopting suitable analysis methods, aimed to monitor the presence of H-bonds and to determine the frequencies of the vibrational modes involved in the interaction at each time step of simulation. In this Letter, we describe the H-bond interaction of methyl acetate (MA) in methanol by a combined use of the H-bond function proposed by Pagliai et al.,[11] and the time−frequency analysis performed within the approach of Torrence and Compo[12] based on wavelet transforms.

MA has a relatively simple molecular structure that makes it an ideal candidate as a case study of the interactions with the surrounding systems. It has been observed in IR spectroscopy that, depending on the nature of the solvent, the vibrational spectrum of MA shows relevant changes, especially in the C═O stretching region.[13] In particular, in CCl_4 and acetonitrile, the C═O stretching mode gives rise to a single band in the infrared spectrum, with the frequency in acetonitrile lower than that in CCl_4. The interactions in water are much more complex; in fact, the C═O stretching band is not only red-shifted with respect to the acetonitrile solution but also shows two well-defined peaks. Candelaresi et al.[13] have recently shown that this behavior is due to the formation of different H-bonded structures, with MA interacting with one or two water molecules. The dynamic equilibrium between the two complexes was characterized by 2D IR spectroscopy in conjunction with Car−Parrinello molecular dynamics (CPMD).[13]

Banno et al.[14,15] recently observed by means of infrared spectroscopy that the C═O stretching band of MA in methanol also splits into a doublet, with a mean frequency higher than that in water solution. On the basis of ab initio calculations and by comparison with the spectra in CCl_4 and water, Banno et al.[14,15] explained this behavior by the setup of an equilibrium between two molecular forms, corresponding to MA involved in zero and one H-bond with the solvent. The presence of a shoulder centered at 1706 cm^{-1} was taken to arise from MA interacting with two methanol molecules. The vibrational relaxation of the C═O stretching mode in the two complexes has been studied by subpicosecond infrared spectroscopy.[14,15]

In order to accurately describe the influence of the H-bond on the structural and spectroscopic properties of MA in methanol, in this Letter, we report on a detailed analysis of the data obtained from CPMD simulations.[16]

The most important structural parameters, related to the H-bond interaction, obtained during the simulations, are summarized in Figure 1.

The H-bond strength depends both on the distance and on the angle. In Figure 1, we report the pair radial and angular distribution functions for MA in methanol (panels a and b) and in water (panels c and d), taken as a reference (the simulation of MA in water has been performed with the same computational

Received Date: August 5, 2010
Accepted Date: September 14, 2010
Published on Web Date: September 20, 2010

DOI: 10.1021/jz1010994 | *J. Phys. Chem. Lett.* **2010**, *1*, 2951–2955

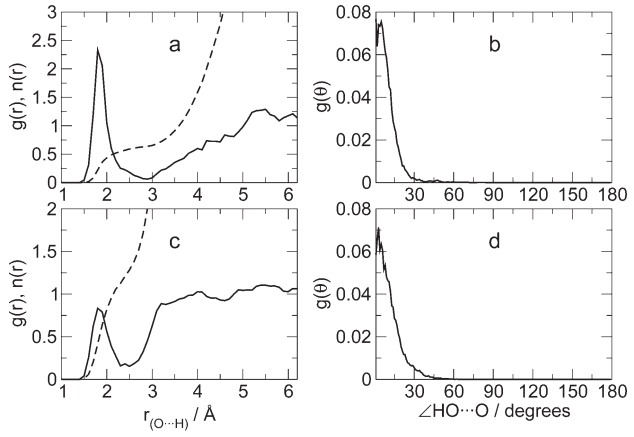

Figure 1. (a) Pair radial distribution function (full line) and running integration number (dashed line) for MA in methanol; (c) the same for MA in water. (b) Angular Distribution function for MA in methanol; (d) the same for MA in water.

approach). In particular, panels a and c show the radial distribution functions for the O···H distances, whereas panels b and d show the distribution function of the HO···O angles limited to the H-bond interactions.

By comparison of the $g(r)$ functions (Figure 1a and c) for MA in the two solvents, some peculiar differences in the H-bond region can be noted, related to the different number of solvent molecules that directly interact with the MA molecule (the coordination number, $n(r)$ in Figure 1a and c). Candelaresi et al.[13] recently reported that the solvation equilibrium of the MA molecule in water corresponds to the formation of one or two H-bonds. In methanol instead, the equilibrium involves two species, with MA forming either zero or one H-bond with the solvent molecules, in agreement with hypothesis of Banno et al.[14,15]. Analyzing the $g(r)$ up to the first minimum (Figure 1a and c), it is possible to correlate the structural parameters with the possibility of a solvent molecule leaving or entering the first solvation shell.[17] For the methanol solution, the minimum of $g(r)$ at about 2.8 Å is much lower than that in the water solution, and correspondently, the height of the first peak is more than twice higher. These two observations indicate that the solvent molecules in the first solvation shell are remarkably more localized in methanol than that in water. In other words, the exchange rate of solvent molecules between the first and second solvation shells is definitely lower in the alcoholic solution. The H-bond formed by MA with methanol is then stronger than that with water. As a consequence of the higher stability of the H-bond interaction, the angular distribution function is sharper in methanol than that in water, as can be observed in Figure 1b and d.

To further clarify this point, a simple model system has been considered, consisting of a MA and one or two solvent molecules. The geometry of the clusters has been optimized with DFT calculations at the BLYP/6-311++G(d,p) level of theory, adopting the Gaussian 03 suite of programs.[18] Figure 2 shows the calculated infrared spectrum of the two clusters in the C═O stretching region. A comparison with the calculated spectra of analogous clusters with water molecules is presented.

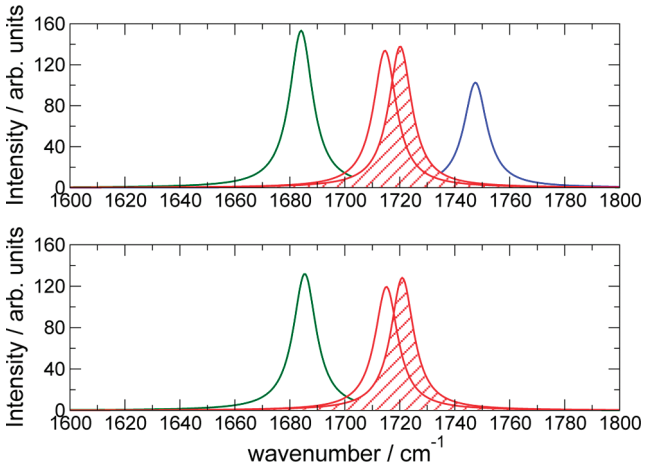

Figure 2. Calculated IR spectra for MA and clusters of MA with one or two methanol (upper panel) and water (lower panel) molecules in the C═O vibrational stretching region. The frequencies have been uniformly scaled by a factor 1.021. Blue, red, and green lines correspond to MA involved in zero, one, and two H-bonds, respectively. The two red bands refer to solvent/MA clusters of different geometry. The calculated spectra have been reported by assigning to each C═O stretching mode a Lorentzian shape with 10 cm^{-1} full width at half-maximum.

It can be seen that the red shift of the infrared band is directly correlated with the number of hydrogen bonds formed. In the case of MA forming one H-bond, two bands are present at slightly different frequencies, corresponding to two distinct minimum structures, with the methanol or water molecules located on opposite sides with respect to the C═O bond.

For an accurate description of the H-bond dynamics of MA in methanol, we adopted for the analysis of our CPMD simulation the hydrogen bond function F^{HB} introduced by Pagliai et al.[11]

The F^{HB} function is defined as

$$F_j^{HB} = A_j(r(t)) \cdot B_j(\theta(t)) \qquad (1)$$

with $A_j(r(t))$ and $B_j(\theta(t))$ given by

$$\begin{cases} A_j(r(t)) = e^{-(r_e - r_j(t))^2/(2\sigma_r^2)} & \text{if } (r_e - r_j(t)) < 0 \\ A_j(r(t)) = 1 & \text{if } (r_e - r_j(t)) \geq 0 \\ B_j(\theta(t)) = e^{-(\theta_e - \theta_j(t))^2/(2\sigma_\theta^2)} & \text{if } (\theta_e - \theta_j(t)) < 0 \\ B_j(\theta(t)) = 1 & \text{if } (\theta_e - \theta_j(t)) \geq 0 \end{cases}$$

The values of the parameters r_e, θ_e, σ_r, and σ_θ are directly extracted from the unnormalized pair radial, $h(r)$, and angular, $h(\theta)$, distribution functions (the H-bond distance and angle distributions found in the simulations). In the above definitions, r_e is the position of the first peak in $h(r)$, and θ_e is the position of the first peak in $h(\theta)$, whereas σ_r and σ_θ are the half widths at half-maximum in $h(r)$ and $h(\theta)$, respectively. The $r_j(t)$ and $\theta_j(t)$ are the instantaneous distance and angle involved in the interaction between the methanol molecule j and the oxygen atom of the C═O group in MA. The F_j^{HB} function assumes values close to 1 for strong H-bond interactions, whereas it goes rapidly to 0 as $r_j(t)$ and $\theta_j(t)$ are larger than the reference values r_e and θ_e. Values of F_j^{HB} lower than 10^{-4} are considered as zeros.

DOI: 10.1021/jz1010994 | J. Phys. Chem. Lett. 2010, 1, 2951–2955

The combined analysis of the F^{HB} function with the instantaneous frequency computed by means of the wavelet transform provides a more descriptive visualization of the H-bond effect on the vibrational frequencies. Wavelet transform allows the simultaneous localization of a time series in the frequency and time domains. The time series analyzed is represented by the variation of the C═O bond length during the CPMD simulation, thus allowing us to compute the frequency of the C═O stretching vibration at each time step of the simulation.

Following the formalism of Torrence and Compo,[12] the wavelet transform of a discrete time series $x_{n'}$ is given by

$$W_n(s) = \sum_{n'=0}^{N-1} x_{n'} \psi^* \left[\frac{(n'-n)\delta t}{s} \right] \quad (2)$$

where s and n are the wavelet scale and the time variation, respectively. The $x_{n'}$ is the time series made up of N observations at δt time intervals, and ψ is the mother wavelet, which, for the subsequent analysis, is given by the Morlet function

$$\psi(t) = \frac{1}{\pi^{1/4}} e^{i\omega_0 t} e^{-t^2/2\sigma^2} \quad (3)$$

where σ is a parameter that determines the resolution of the spectrum.

To reduce the computational time required to calculate the wavelet transforms, we solved eq 2 in the reciprocal space using the equation

$$W_n(s) = \sum_{k=0}^{N-1} \hat{x}_k \hat{\psi}^*(s\omega_k) e^{i\omega_k n \delta t} \quad (4)$$

where k is the frequency index, ω_k is the angular frequency, and $\hat{x}_k$ and ψ are the Fourier transforms of $x_{n'}$ and ψ, respectively.

The wavelet analysis of the C═O stretching vibrational mode allows one to obtain more information compared to standard Fourier analysis and can be of valuable help in the spectroscopic and structural characterization of the H-bond of MA in methanol solution. Figure 3 shows the analysis performed with wavelet transforms in conjunction with the F^{HB} function. The result gives a clear description of the response of the C═O stretching mode to the variation of the H-bond strength.

The presence of the H-bond interaction can be appreciated from the F^{HB} function reported in panel a of Figure 3. It can be seen that a hydrogen bond is present only in the first ~4 ps of the simulation with molecule 58 of the solvent and after ~12 ps with molecule 2. The behavior of the F^{HB} function (F_2^{HB} and F_{58}^{HB}) shows the importance of a continuous function for characterizing the H-bond, like F^{HB}, which accounts for the fast oscillation in and out of the geometrical constraints usually taken as a probe of the formation of a H-bond. In fact (see panel b of Figure 3), as long as the H-bonded molecule resides in the first solvation shell, the fast modulation of the C═O stretching frequency takes place at around 1719 cm^{-1} (red dashed horizontal line). Instead, when no methanol molecule is H-bonded with MA, the C═O frequency occurs

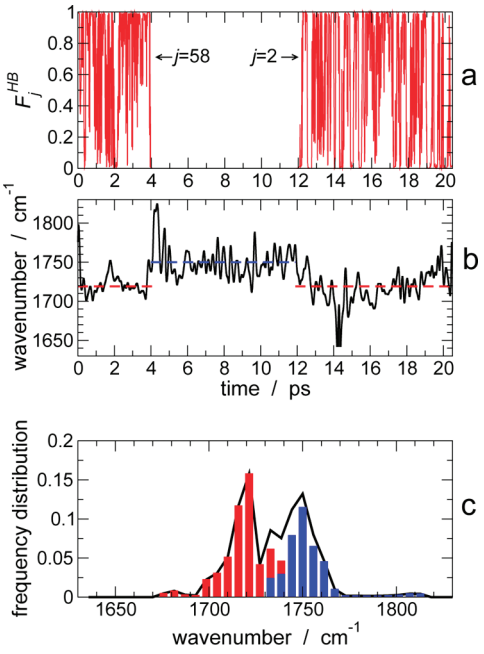

Figure 3. (a) Evolution of F_j^{HB} for the molecule with j = 2 and 58. A molecule with j = 58 forms a H-bond in the first part of the simulation, whereas a molecule with j = 2 interacts with MA in the last part of the simulation. (b) Time evolution of the maximum of the C═O stretching band during the simulation. The dashed lines represent the average frequency of the C═O stretching mode in the presence (red) or absence (blue) of the H-bond. (c) C═O stretching frequency distribution for MA during the simulation. The red and blue bars indicate the frequency distribution of MA involved and not involved in H-bond interaction, respectively. The frequencies have been uniformly scaled by a factor of 1.095.

at a higher wavenumber of 1750 cm^{-1} (blue dashed line). The interaction with the solvent molecules induces a red shift in the C═O stretching frequency of about 30 cm^{-1}, a value slightly higher than that experimentally observed.[14,15] Although no double H-bond configurations have been observed during the simulation, in some cases, a second molecule approaches MA, entering the first solvation shell region. This corresponds to the low-frequency shoulder observed in the experimental spectrum. The C═O stretching frequency distribution can be appreciated in panel c of Figure 3, showing a bandwidth close to that measured in infrared spectra.[14,15] An attempt to calculate the H-bond lifetime has been performed by computing the correlation function of F^{HB}, obtaining an estimate on the order of 1 ps, which compares with the experimental relaxation time.[14,15] We have applied other methods to compute the H-bond lifetime according to the definition given in ref 11; the order of magnitude of the lifetime does not change, ranging in the values between ~0.5 and ~2 ps.

An alternative approach to correlate the results obtained from the F^{HB} function with the vibrational frequencies of the C═O stretching mode of MA can be accomplished by taking advantage of the time localization capability of wavelet transforms. Actually, by this technique, it is possible to extract at each time step of the simulation the C═O bond length and the corresponding vibrational frequency. Thus, we can draw a

DOI: 10.1021/jz1010994 | J. Phys. Chem. Lett. 2010, 1, 2951–2955

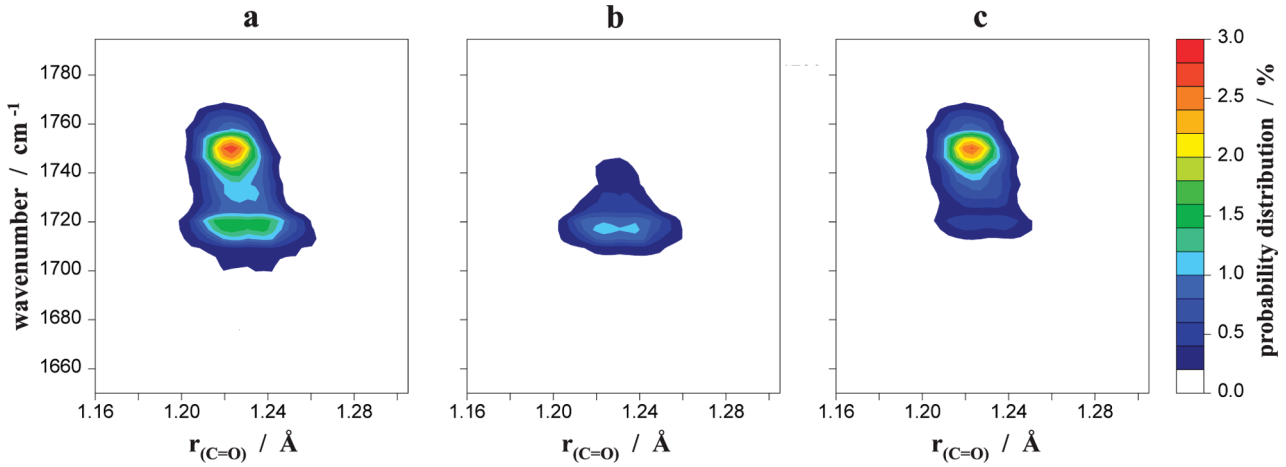

Figure 4. (a) Probability distribution of the C═O stretching mode as a function of the C═O bond length. Panels (b) and (c) represent the probability distribution given in (a), weighted by F^{HB} and $(1 - F^{HB})$ factors, respectively. The frequencies have been uniformly scaled by a factor of 1.095.

two-dimensional plot in which the distribution of the instantaneous frequencies is expressed in terms of a specific structural parameter. Figure 4a shows the probability distribution of the C═O stretching frequency as a function of C═O bond length. As expected, the surface is characterized by the presence of two main regions, with the maxima separated by ~30 cm^{-1}, corresponding to MA being or not being involved in the H-bond interaction. It is interesting to note that the shape of the two regions is quite different; this allows one to pinpoint the correspondence between structural changes and frequency values. The presence of the H-bond not only leads to a red shift of the C═O stretching mode frequency but also makes the C═O bond span a larger length range. This behavior can be better appreciated in Figure 4b and c, where a clear separation of the two spectral regions is obtained by weighting the probability distribution by F^{HB} and $(1 - F^{HB})$, respectively.

The possibility to localize the vibrational modes in the time and frequency domain by wavelet transform makes molecular dynamics simulations particularly effective in the study of H-bond dynamics and helpful in the comprehension of the experimental results obtained with time-resolved spectroscopies.

COMPUTATIONAL METHOD

The simulations were performed on a system made up of 1 MA and 64 fully deuterated methanol molecules in a periodic cubic box with sides of 16.3095 Å. A BLYP exchange and correlation functional[19,20] was employed along with norm-conserving Martins-Troullier[21] pseudopotentials within the Kleinman−Bylander[22] decomposition. The plane wave expansion was truncated at 85 Ry, while the fictitious electronic mass was 600 au. The system was thermalized at 300 K for 2.6 ps by velocity scaling. The simulation (in the NVE ensemble) was ~20 ps long, saving the coordinates at each integration time step of 5 au (~0.12 fs). The average temperature was 315 ± 10 K.

The simulations in water have been performed with the same parameters reported in Candelaresi et al.,[13] with the exception of the plane wave expansion truncated at 85 Ry. For a correct comparison of the results, the simulation length is the same as that for MA in methanol.

AUTHOR INFORMATION

Corresponding Author:

*To whom correspondence should be addressed. E-mail: gianni.cardini@unifi.it.

ACKNOWLEDGMENT This work was supported by the Ministero dell'Istruzione, dell'Università e della Ricerca (MIUR). The authors would like to thank the CINECA Supercomputing Center for the allocation of computing resources.

REFERENCES

(1) Fayer, M. D. Dynamics of Liquids, Molecules, and Proteins Measured with Ultrafast 2D IR Vibrational Echo Chemical Exchange Spectroscopy. *Annu. Rev. Phys. Chem.* **2009,** *60*, 21–38.
(2) Kim, Y. S.; Hochstrasser, R. M. Applications of 2D IR Spectroscopy to Peptides, Proteins, and Hydrogen-Bond Dynamics. *J. Phys. Chem. B* **2009,** *113*, 8231–8251.
(3) Woutersen, S.; Hamm, P. Nonlinear Two-Dimensional Vibrational Spectroscopy of Peptides. *J. Phys.: Condens. Matter* **2002,** *14*, R1035–R1062.
(4) Zhuang, W.; Hayashi, T.; Mukamel, S. Coherent Multidimensional Vibrational Spectroscopy of Biomolecules: Concepts, Simulations, and Challenges. *Angew. Chem., Int. Ed.* **2009,** *48*, 3750–3781.
(5) Cho, M. Coherent Two-Dimensional Optical Spectroscopy. *Chem. Rev.* **2008,** *108*, 1331–1418.
(6) Ladanyi, B. M.; Skaf, M. S. Computer Simulation of Hydrogen-Bonding Liquids. *Annu. Rev. Phys. Chem.* **1993,** *44*, 335–368.
(7) Car, R.; Parrinello, M. Unified Approach for Molecular Dynamics and Density-Functional Theory. *Phys. Rev. Lett.* **1985,** *55*, 2471–2474.
(8) Parrinello, M. From Silicon to RNA: the Coming of Age of *Ab Initio* Molecular Dynamics. *Solid State Commun.* **1997,** *102*, 107–120.
(9) Tse, J. S. Ab Initio Molecular Dynamics with Density Functional Theory. *Annu. Rev. Phys. Chem.* **2002,** *53*, 249–290.
(10) Marx, D.; Hutter, J. *Ab Initio Molecular Dynamics*; Cambridge University Press, 2009.
(11) Pagliai, M.; Cardini, G.; Righini, R.; Schettino, V. Hydrogen Bond Dynamics in Liquid Methanol. *J. Chem. Phys.* **2003,** *119*, 6655–6662.

DOI: 10.1021/jz1010994 | *J. Phys. Chem. Lett.* **2010,** *1*, 2951–2955

(12) Torrence, C.; Compo, G. P. A Practical Guide to Wavelet Analysis. *Bull. Am. Meteorol. Soc.* **1998,** *79*, 61–78.
(13) Candelaresi, M.; Pagliai, M.; Lima, M.; Righini, R. Chemical Equilibrium Probed by Two-Dimensional IR Spectroscopy: Hydrogen Bond Dynamics of Methyl Acetate in Water. *J. Phys. Chem. A* **2009,** *113*, 12783–12790.
(14) Banno, M.; Ohta, K.; Yamaguchi, S.; Hirai, S.; Tominaga, K. Vibrational Dynamics of Hydrogen-Bonded Complexes in Solutions Studied with Ultrafast Infrared Pump−Probe Spectroscopy. *Acc. Chem. Res.* **2009,** *42*, 1259–1269.
(15) Banno, M.; Ohta, K.; Tominaga, K. Ultrafast Vibrational Dynamics and Solvation Complexes of Methyl Acetate in Methanol Studied by Sub-Picosecond Infrared Spectroscopy. *J. Raman Spectrosc.* **2008,** *39*, 1531–1537.
(16) *CPMD*, Copyright IBM Corp 1990−2008, Copyright MPI für Festkörperforschung Stuttgart 1997−2001; http://www.cpmd.org.
(17) The accuracy of the $g(r)$ has been checked by performing subaverages, without observing differences in the positions of the first maximum and minimum. The H-bond evolution differs in time in the two subaverages, inducing slight changes in the first peak height and in the value of the minimum deep in the $g(r)$.
(18) Frisch, M. J.; Trucks, G. W.; Schlegel, H. B.; Scuseria, G. E.; Robb, M. A.; Cheeseman, J. R.; Montgomery, Jr., J. A.; Vreven, T.; Kudin, K. N.; Burant, J. C.; et al. *Gaussian 03*, revision C.02; Gaussian, Inc.: Wallingford CT, 2004.
(19) Becke, A. D. Density-Functional Exchange-Energy Approximation with Correct Asymptotic Behavior. *Phys. Rev. A* **1988,** *38*, 3098–3100.
(20) Lee, C.; Yang, W.; Parr, R. G. Development of the Colle−Salvetti Correlation-Energy Formula into a Functional of the Electron Density. *Phys. Rev. B* **1988,** *37*, 785–789.
(21) Troullier, N.; Martins, J. L. Efficient Pseudopotential for Plane-Wave Calculations. *Phys. Rev. B* **1991,** *43*, 1993–2006.
(22) Kleinman, L.; Bylander, D. M. Efficacious Form for Model Pseudopotentials. *Phys. Rev. Lett.* **1982,** *48*, 1425–1428.

DOI: 10.1021/jz1010994 | *J. Phys. Chem. Lett.* **2010,** *1*, 2951–2955